Measurement of conservative and dissipative tip-sample interaction forces with a dynamic force microscope using the frequency modulation technique

H. Hölscher,[1,*] B. Gotsmann,[2,†] W. Allers,[1,*] U. D. Schwarz,[1,‡] H. Fuchs,[2] and R. Wiesendanger[1]
[1]*Institute of Applied Physics, University of Hamburg, Jungiusstr. 11, 20355 Hamburg, Germany*
[2]*Institute of Physics, University of Münster, Wilhelm-Klemm-Str. 10, 48149 Münster, Germany*
(Received 15 February 2001; published 13 July 2001)

The measurement principle of dynamic-force microscopy using the frequency-modulation (FM) detection scheme is investigated by analytical as well as numerical approaches. As the detection method is based on the properties of a self-driven oscillator, we discuss the main differences from an externally driven oscillator. We then derive an analytical expression, which clarifies how the measured quantities of the FM technique, the frequency shift, and the gain factor (or ''excitation amplitude'') are influenced by the time (''phase'') shift. Introducing a very general tip-sample force law, we show that the frequency shift is determined by the mean tip-sample force whereas the gain factor is directly related to dissipative processes like hysteresis or viscous damping.

DOI: 10.1103/PhysRevB.64.075402 PACS number(s): 68.37.Ps, 07.79.Lh, 87.64.Dz

I. INTRODUCTION

Since the design of the first atomic-force microscope (AFM) by Binnig, Quate, and Gerber in 1986,[1] this microscopy method has been established as a standard tool in surface physics. Nonetheless, it took several years until the imaging of single-point defects, i.e., ''true'' atomic resolution, was achieved using dynamic force microscopy (DFM), which is often also termed as noncontact atomic-force microscopy (NC-AFM).[2,3] Since then, the field of DFM/NC-AFM has been growing rapidly, and true atomic resolution has been obtained on many different types of surfaces including conductors, semiconductors, and insulators.[4]

Parallel to the experimental progress, theoretical studies were performed in order to analyze the information that can be extracted from DFM experiments. Much of this effort focused on the description of setups based on *externally driven* oscillators, which have been widely investigated by numerical as well as analytical approaches (see, e.g., Refs. 5–13). However, since high-resolution experiments need clean sample surfaces, they are usually performed in ultrahigh vacuum (UHV). Consequently, most DFM's use the frequency modulation (FM) detection scheme introduced by Albrecht *et al.*,[14] which is much better suited for vacuum conditions, but is based on the excitation principle of a *self-driven* oscillator. The specific properties of such an oscillator have only been analyzed by numerical simulations up to now.[15–17]

Therefore, it is the aim of this work to study the specific features of experimental setups based on the FM detection scheme. To begin with, we describe the differences between an externally driven and a self-driven cantilever in Sec. II. General aspects of a self-driven cantilever without any tip-sample interaction force are discussed in Sec. III to clarify the basic properties of this driving method. Finally, conservative and dissipative tip-sample forces are considered in Sec. IV to show how experimental results obtained with the FM technique can be interpreted.

II. DRIVEN AND SELF-DRIVEN CANTILEVERS IN DYNAMIC ATOMIC-FORCE MICROSCOPY

Atomic-force microscopes using detection schemes working with a vibrating cantilever (''dynamic'' modes of operation) are often based on an experimental setup where the cantilever is driven by an external oscillator with a fixed excitation frequency, if they are run under ambient conditions. The equation of motion of the cantilever is then given by the differential equation of a driven damped oscillator with the (nonlinear) tip-sample force F_{ts} (Refs. 5–13),

$$m\ddot{z}(t)+\frac{2\pi f_0 m}{Q}\dot{z}(t)+c_z z(t) = F_{\mathrm{ts}}[z(t),\dot{z}(t)]+\underbrace{a_d c_z \cos(2\pi f_d t)}_{\text{external excitation}}, \tag{1}$$

where $z(t)$ is the position of the tip at the time t; c_z, m, Q, and $f_0=\sqrt{(c_z/m)}/(2\pi)$ are the spring constant, the effective mass, the quality factor, and the eigenfrequency of the cantilever, respectively. The external excitation of the cantilever with the excitation amplitude a_d at a fixed frequency f_d is described by the term on the right side of Eq. (1).

The solutions of this nonlinear equation of motion are oscillations, which have been examined for a long time and might be quite complex.[8,9] In dynamic force microscopy, however, one is mainly interested in steady-state solutions, where the cantilever oscillations are nearly sinusoidal. In this case, the oscillation frequency is given by the external frequency f_d, and the solution of Eq. (1) is given by

$$z(t\gg 0)\cong A(f_d,a_d)\cos[2\pi f_d t+\phi_0(f_d,a_d)], \tag{2}$$

where the oscillation amplitude and the phase shift are functions of the excitation frequency and the excitation amplitude. The explicit form of these functions depends on the tip-sample interaction force F_{ts}.[8] Thus, different detection schemes, which use either the oscillation amplitude A or the

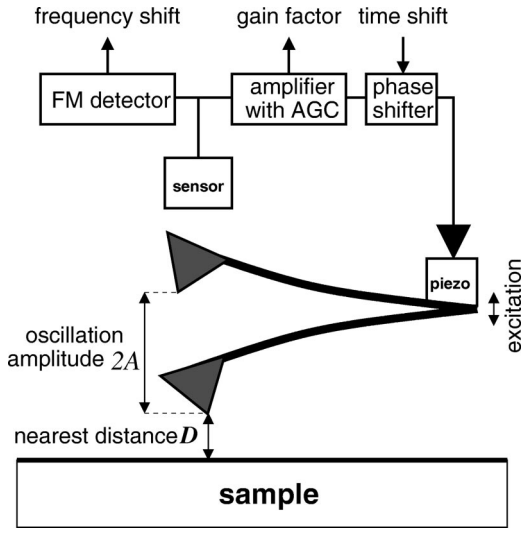

FIG. 1. The schematic setup of a dynamic-force microscope operated in UHV using the frequency-modulation technique (constant-amplitude mode) introduced by Albrecht *et al.*[14] A significant feature of this setup is the positive feedback of the self-driven cantilever (see text).

phase shift ϕ for distance control, have been established for dynamic atomic-force microscopes with an externally driven cantilever.[18]

However, as it has been pointed out by Albrecht *et al.*,[14] an experimental setup based on an externally driven cantilever has a principle limitation of the sensitivity if it is run in ultra-high vacuum. Due to the high Q values of AFM cantilevers in UHV ($Q \approx 10\,000 - 100\,000$), the response of the system during data acquisition is very slow, restricting the bandwith of the experimental setup.

This problem does not exist for the frequency modulation technique,[14] where the sensitivity of the microscope increases with the Q value of the cantilever. Consequently, this detection scheme is commonly used for dynamic-force microscopes working in UHV. As mentioned in the Introduction, most NC-AFM/DFM experiments with high resolution must be done under well-defined conditions in ultrahigh vacuum. In fact, ''true'' atomic resolution has been obtained up to now only on clean surfaces in UHV using dynamic modes, where the tip is believed to vibrate without touching the sample surface (''noncontact'' AFM). Thus, we will investigate the FM detection scheme in the following.

The key feature of FM detection is the positive feedback, which ensures that the cantilever oscillates always at its resonance frequency. The reason for this behavior is that the cantilever serves as the frequency-determining element. This is in contrast to an externally driven cantilever: Such a cantilever oscillates in steady state with its excitation frequency, which is not necessarily its resonance frequency [see Eq. (2)].

A schematic setup of a DFM using the FM technique is shown in Fig. 1. The movement of the cantilever is measured with a displacement sensor. This signal is then fed into an amplifier possessing an automatic gain control (AGC) and is subsequently used to excite the piezo driving the cantilever. The phase shift between the excitation signal and cantilever deflection is adjusted by a phase (or time) shifter to a value corresponding to $\approx 90°$, since this ensures an oscillation near resonance (see Sec. III). Two different modes have been established for use with the FM detection: The *constant-amplitude mode*, where the oscillation amplitude is kept at a constant value by the AGC,[14] and the *constant-excitation mode*,[19] where the excitation amplitude is kept constant. In this article, however, we focus on the original constant-amplitude mode.

With such an experimental setup, the corresponding equation of motion of an AFM with FM technique driven in the constant amplitude mode is different from Eq. (1). It is now a differential equation with a time delay[15–17] t_0,

$$m\ddot{z}(t) + \frac{2\pi f_0 m}{Q}\dot{z}(t) + c_z z(t) = F_{\mathrm{ts}}[z(t), \dot{z}(t)] + \underbrace{g\, c_z z(t - t_0)}_{\text{driving}}. \tag{3}$$

The term on the right side of this equation differs from the external driving term in Eq. (1) and describes the active feedback of the system by the amplification of the displacement signal, i.e., the tip position z measured at the retarded time $t - t_0$ by the gain factor g.

Due to the obvious difference in the equations of motion of the driven and the self-driven oscillator, it is quite clear that both have different features that have to be taken into account for the analysis of experimental data. To give insight into the properties of a self-driven oscillator, we discuss the solutions of Eq. (3) with and without tip-sample force in the following sections.

III. SELF-DRIVEN CANTILEVER *WITHOUT* TIP-SAMPLE INTERACTION FORCE

To study the basic behavior of a self-driven oscillator we assume that the cantilever vibrates far away from the sample surface. In this case, there are no tip-sample forces ($F_{\mathrm{ts}} \equiv 0$) and Eq. (3) simplifies to

$$m\ddot{z}(t) + \frac{2\pi f_0 m}{Q}\dot{z}(t) + c_z z(t) = g\, c_z z(t - t_0). \tag{4}$$

For the analysis of experiments, we are only interested in steady-state solutions for $t \gg 0$, where the cantilever oscillations are sinusoidal and the amplitude is constant. Therefore, we make the ansatz

$$z(t \gg 0) = A\cos(2\pi f t), \tag{5}$$

introduce it into Eq. (4), and finally get a set of two coupled trigonometric equations,

$$g\cos(2\pi f t_0) = \frac{f_0^2 - f^2}{f_0^2}, \tag{6a}$$

$$g\sin(2\pi f t_0) = -\frac{1}{Q}\frac{f}{f_0}. \tag{6b}$$

Since the amplitude A is held constant by the AGC and the time delay t_0 is a constant value set by the phase shifter, Eq. (6) must be solved for the oscillation frequency f and the gain factor g. However, before analyzing the general solution we examine the behavior of the system at resonance.

In this case, the trigonometric equations (6) can be simplified and decoupled with the assumption that the time shift t_0 is set to a value corresponding to

$$t_0 = \underbrace{\tfrac{1}{4}T_0}_{=90^\circ},\ \underbrace{\tfrac{3}{4}T_0}_{=270^\circ},\ \underbrace{\tfrac{5}{4}T_0}_{=450^\circ},\ldots, \tag{7}$$

where $T_0 = 1/f_0$ is the period of oscillation of the free and undamped cantilever. For these values of t_0, the solution of Eq. (6) is given by

$$f = f_0, \tag{8a}$$

$$|g| = 1/Q. \tag{8b}$$

These simple calculations demonstrate the interesting and very specific behavior of a self-driven oscillator with velocity-dependent damping: The cantilever oscillates exactly with its eigenfrequency f_0 and the gain factor g depends only on the Q value of the cantilever if the time delay is set to a value given by Eq. (7). Consequently, we define that the system is in resonance, if Eq. (7) is fulfilled.

In a real experiment, the time (or phase) shift between the excitation and the cantilever oscillations might be slightly detuned. Consequently, it is necessary to examine the impact of this effect on the oscillation frequency f and the gain factor g. We do this in two different ways. First, we present an approximate (but handy) analytical solution of Eq. (6), which might be valuable for experimentalists to calculate the errors caused by a detuned time shift t_0. Then we compare this result with the numerical simulation of the experimental setup based on the numerical solution of Eq. (3) (Refs. 15–17).

If the time delay is not given by the special values of Eq. (7), the system is out of resonance and the oscillation frequency shifts from the eigenfrequency of the cantilever by $\Delta f_{\mathrm{err}} := f - f_0$. The gain factor differs also from the value given by Eq. (8b). The general behavior of the system can in this case be analyzed by the following approximate solution of Eq. (6): Since the frequency error is quite small ($\Delta f_{\mathrm{err}} \ll f_0$) for a small detuning of t_0, it can be shown that

$$\Delta f_{\mathrm{err}} \approx \frac{f_0}{2Q}\cot(2\pi f_0 t_0), \tag{9a}$$

$$|g| \approx \frac{1}{Q}\frac{1}{\sin(2\pi f_0 t_0)}. \tag{9b}$$

These two functions are plotted in Fig. 2 for typical parameters by solid lines. The left axis of the graph represents the values of the frequency error and the gain factor. (For our purposes, the sign of the gain factor can be arbitrarily defined, therefore we plot only its absolute value $|g|$.) The percental deviation from the optimal value at 90° is shown on the right axis. The corresponding values obtained from a numerical simulation of the whole system are marked by symbols. The excellent agreement between the simulation and the analytical solution demonstrates the reliability of both approaches to solve Eq. (4).

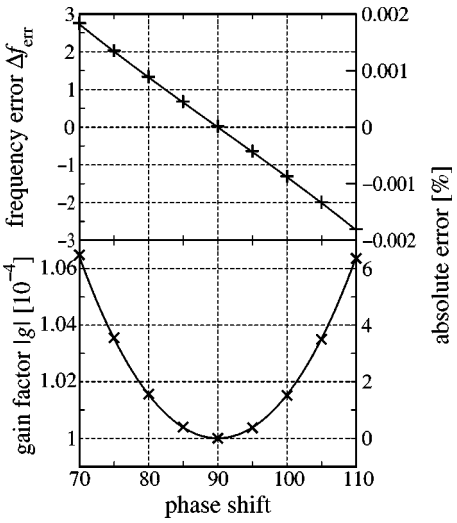

FIG. 2. The shift of the frequency Δf_{err} and the gain factor g without a tip-sample force as a function of the phase shift, i.e., the time delay t_0, t_0 for the parameters: $f_0 = 150$ kHz, $c_z = 40$ N/m, $A = 100$ Å, and $Q = 10\,000$. The solid lines and the symbols mark the solution of Eq. (9) and the numerical simulation of the whole system, respectively. The left axis represents the shift of the frequency and the gain factor from the resonance values at 90°; the right axis shows the corresponding error.

Figure 2 and the analysis of Eq. (9) demonstrate that the frequency error caused by an improper adjustment of t_0 changes nearly linearly with the time delay and is quite small. Even for a large detuning of 20° the error is smaller than 0.002 %. The change in the gain factor is much larger than the frequency error: A detuning of 10° (20°) leads to an error of about 2% (6%). The absolute value of the gain factor, however, minimizes if the system is in resonance and varies parabolically with t_0 if the system is out of resonance. Therefore, it is straightforward to determine the optimal values for t_0 in an experiment. If the cantilever is far away from the sample surface (i.e., zero tip-sample force), the optimal value for the time delay can easily be found by a minimization of the gain factor as a function of t_0.

IV. SELF-DRIVEN CANTILEVER *WITH* TIP-SAMPLE INTERACTION FORCE

It is the main purpose of an atomic-force microscope to measure tip-sample interaction forces. Consequently, it is elementary to analyze the influence of the tip-sample interaction on the resonance frequency and the gain factor. This can be done either by numerical simulations[15–17] or by the analysis of the equation of motion (3). For both approaches it can be assumed that the tip-sample interaction force is a function of the actual tip position $z(t)$ and its velocity $\dot{z}(t)$ ($\Rightarrow F_{\mathrm{ts}}$

$:=F_{ts}[z(t),\dot{z}(t)]$). The exact form of this function, however, depends on many different parameters such as the material properties of tip and sample, the shape of the tip, the bias voltage, etc.

For such a force, the equation of motion Eq. (3) can again be solved with the ansatz Eq. (5). Then, the obtained equation is simplified in the following way:[20] After a multiplication with $\cos(2\pi ft)$, the equation is integrated over one period of oscillation $t=[0,1/f]$. The same procedure is repeated after a multiplication with $\sin(2\pi ft)$. The result is a set of two coupled trigonometric equations,

$$g\cos(2\pi f t_0)=\frac{f_0^2-f^2}{f_0^2}-\frac{2f}{Ac_z}\int_0^{1/f}F_{ts}[z(t),\dot{z}(t)]\cos(2\pi ft)\,dt, \tag{10a}$$

$$g\sin(2\pi f t_0)=-\frac{1}{Q}\frac{f}{f_0}-\frac{2f}{Ac_z}\int_0^{1/f}F_{ts}[z(t),\dot{z}(t)]\sin(2\pi ft)\,dt. \tag{10b}$$

These equations may be solved numerically to determine the exact dependency of the tip-sample interaction force F_{ts} and the time delay t_0 on the oscillation frequency f and the gain factor g.

The detailed analysis, however, demonstrates that the results of a DFM experiment are mainly determined by the tip-sample force and only slightly by the time delay. This can be shown by an approximation of Eq. (10), which is based on the assumption that condition Eq. (7) is fulfilled. In this case, the time delay is set to an optimal value by the experimentalist before an approach of the tip towards the sample surface (see Sec. III). Since the frequency shifts caused by the tip-sample interaction are usually quite small, the system is also nearly in resonance during the measurement of tip-sample forces. Therefore, it can be assumed that $\cos(2\pi ft_0)\approx 0$ and $\sin(2\pi ft_0)\approx\pm 1$.

With this assumption the two coupled equations (10a) and (10b) can be decoupled and we obtain

$$\Delta f\cong-\frac{f_0^2}{Ac_z}\int_0^{1/f_0}F_{ts}[z(t),\dot{z}(t)]\cos(2\pi f_0 t)\,dt, \tag{11a}$$

$$|g|\cong\frac{1}{Q}+\frac{2f_0}{Ac_z}\int_0^{1/f_0}F_{ts}[z(t),\dot{z}(t)]\sin(2\pi f_0 t)\,dt. \tag{11b}$$

Since we did not make any assumption about the specific force law describing the tip-sample interaction F_{ts}, these equations are valid for every type of interaction as long as the resulting cantilever oscillations are nearly sinusoidal. In

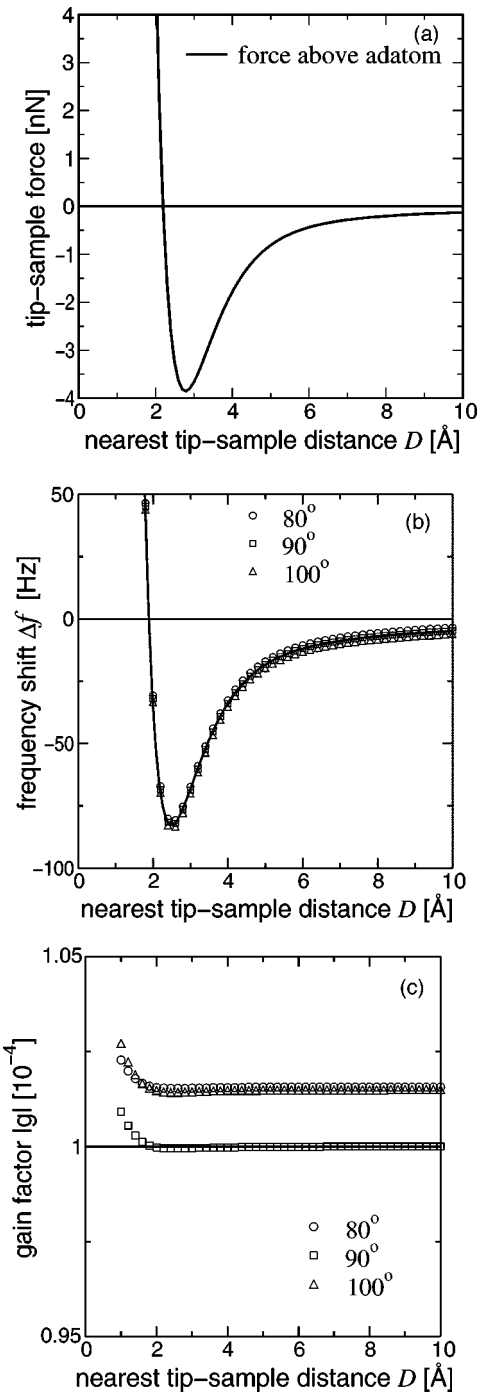

FIG. 3. (a) The tip-sample force between an adatom of the Si(111)(5×5) surface after Peréz *et al.* (Ref. 23). (b) The frequency shift caused by the tip-sample force shown in (a). The solid line is the result of Eq. (11a). The symbols represent the numerical simulations calculated with different time delays t_0. The parameters are the same as in Fig. 2: $f_0=150$ kHz, $c_z=40$ N/m, $A=100$ Å, and $Q=10\,000$. (c) The gain factor corresponding to the results shown in (b). Since the used tip-sample force is purely conservative, the solution of Eq. (11b) is a constant value $|g|=1/Q=10^{-4}$ (solid line). The comparison with the numerical simulations for different time delays t_0 (symbols) shows that the precision of this approximated formula is better than 3%.

this context, it is interesting to note that Eq. (11a) coincides with the well-known result of Refs. 21 and 22 if F_{ts} is a conservative force.

To demonstrate the reliability of these formulas we compared them with numerical simulations of the system based on Eq. (3) using a purely conservative tip-sample force as shown in Fig. 3(a). It describes the short- and long-range interaction between an atomically sharp silicon tip and an adatom of the Si(111) (5×5) surface as calculated by Peréz *et al.*[23] The corresponding frequency shift is displayed in Fig. 3(b). The solid line is calculated from Eq. (11a). The symbols represent the results of numerical simulations if the system is in resonance (90°) and for detuned time delays (80°,100°). For resonance, the error of the approximation Eq. (11a) is negligible. For a detuning of 10° it is smaller than 5 Hz. The approximation for the gain factor is also quite reasonable [see Fig. 3(c)]. The calculation with Eq. (11b) gives a constant value $|g|=1/Q$, which depends only on the quality factor of the cantilever, since the integral on the right side is zero for conservative tip-sample forces. The deviation from the numerically obtained gain factor values can be neglected at resonance and it is smaller than 3% for a detuning of 10°.

This example shows that a conservative tip-sample force influences mainly the frequency shift but not the gain factor, which is nearly constant. All deviations displayed in Fig. 3(c) are small effects mainly caused by the detuning of the time shift. However, experimental NC-AFM data obtained with the FM detection scheme show typically much larger variations of the gain factor towards the sample surface.[17] Various authors suggested physical mechanisms[24] and dissipative force laws[17,25] to explain this behavior. Even though it is beyond the scope of this article to examine the physical significance of these approaches, we adopt our equations for the frequency shift and the gain factor to a force law including dissipation.

For this purpose, we assume the following force law to describe the tip-sample interaction

$$F_{ts} := F_{int}(z) + F_{diss}(z,\dot{z}), \tag{12}$$

where the first term depends only on the tip-sample position and the actual movement direction of the tip

$$F_{int}(z) := \begin{cases} F_{\rightarrow}(z), & \dot{z} \leqslant 0 \quad \text{``forward''} \\ F_{\leftarrow}(z), & \dot{z} > 0 \quad \text{``backward,''} \end{cases} \tag{13}$$

while the second term describes the energy dissipation due to a viscous damping

$$F_{diss}(z,\dot{z}) := \gamma_1(z)\,\dot{z}, \tag{14}$$

where the damping coefficient γ is a function of the actual tip position.

For the application of these force laws to Eqs. (11) it is convenient to use the transformation $z(t) := A\cos(2\pi f_0 t)$ for the simplification of the integrals on the right side of these equations. We then find

$$\Delta f \cong -\frac{f_0}{\pi A^2 c_z}\int_{-A}^{A} \frac{F_{\rightarrow}+F_{\leftarrow}}{2}\,\frac{z}{\sqrt{A^2-z^2}}\,dz, \tag{15a}$$

$$|g| \cong \frac{1}{Q} + \frac{1}{\pi A^2 c_z}\int_{-A}^{A}(F_{\rightarrow}-F_{\leftarrow})\,dz + \frac{4f_0}{A^2 c_z}\int_{-A}^{A}\gamma_1(z)\sqrt{A^2-z^2}\,dz. \tag{15b}$$

This result demonstrates that the frequency shift depends only on the *average of the tip-sample force* between forward and backward movement, but is *independent* of the dissipative force Eq. (14). In contrast, the gain factor g is directly related to all energy-dissipation processes: The intrinsic damping of the cantilever leads to a constant term $1/Q$. The second term is given by an integral over the difference of the tip-sample force between forward and backward movement, i.e., the hysteresis, whereas the third term is related to the viscous damping mechanism.

V. SUMMARY

In summary, we analyzed the measurement principle of dynamic-force microscopy using the FM technique in the constant-amplitude mode. It was found that due to the specific-excitation principle based on a self-driven oscillator, the cantilever oscillates exactly with its eigenfrequency for a time delay corresponding to 90°. This is in contrast to the conventional externally driven oscillator. As shown by analytical and numerical calculations, the necessary adjustment of the time delay can easily be performed by the minimization of the gain factor.

Additionally, general analytic equations determining the frequency shift and the gain factor for arbitrary tip-sample forces could be derived, which are valid as long as the cantilever oscillations are nearly sinusoidal. With the assumption of a force law describing the energy dissipation between tip and sample by hysteresis and/or viscous damping, we could finally show that the frequency shift is given by the mean tip-sample force whereas the gain factor is directly related to dissipative forces.

ACKNOWLEDGMENTS

The authors gratefully acknowledge financial support from the Deutsche Forschungsgemeinschaft (Grants Nos. FU 299/8-1, SCHW641/1-1, and WI 1277/13) and the BMBF (Grant No. 13N7694/8).

*Present address: Infineon Technologies, St. Martin Strasse 76, 81541, Munich, Germany.

†Present address: IBM Research Division, Zurich Research Laboratory, CH-8803, Ruschilkon, Switzerland.

‡Present address: Lawrence Berkeley National Laboratory, Materials Science Division (Bldg. 66), University of California, 1 Cyclotron Road, Berkeley, CA 94720.

[1] G. Binnig, C. F. Quate, and Ch. Gerber, Phys. Rev. Lett. **56**, 930 (1986).

[2] F.-J. Giessibl, Science **267**, 68 (1995).

[3] Y. Sugawara, M. Otha, H. Ueyama, and S. Morita, Science **270**, 1646 (1995).

[4] An overview on the recent developments in noncontact atomic-force microscopy can be found in NC-AFM 1998, Proceedings of the International Conference on Non-Contact Atomic Force Microscopy, edited by S. Morita and M. Tsukada [Appl. Surf. Sci. **140**, 243 (1999)]; NC-AFM 1999, Proceedings of the International Conference on Non-Contact Atomic Force Microscopy, edited by R. Bennewitz, Ch. Gerber, and E. Meyer [*ibid.* **157**, 207 (2000)]; NC-AFM 2000, Proceedings of the International Conference on Non-Contact Atomic Force Microscopy, edited by U. D. Schwarz, H. Hölscher, and R. Wiesendanger [Appl. Phys. A (to be published)].

[5] B. Ancykowski, D. Krüger, and H. Fuchs, Phys. Rev. B **53**, 15 485 (1996).

[6] A. Kühle, A. H. Sørensen, and J. Bohr, J. Appl. Phys. **81**, 6592 (1997).

[7] D. Krüger, B. Anczykowski, and H. Fuchs, Ann. Phys. (Leipzig) **6**, 34 (1997).

[8] N. Sasaki and M. Tsukada, Jpn. J. Appl. Phys., Part 2 **37**, L533 (1998).

[9] N. Sasaki, M. Tsukada, R. Tamura, K. Abe, and N. Sato, Appl. Phys. A: Mater. Sci. Process. **A66**, S287 (1998).

[10] O. Behrendt, F. Oulevey, D. Gourdon, E. Dupas, A. J. Kulik, G. Gremaud, and N. A. Burnham, Appl. Phys. A: Mater. Sci. Process. **A66**, S219 (1998).

[11] M. Labardi, Probe Microsc. **1**, 215 (1998).

[12] R. Boisgard, D. Michel, and J. P. Aime, Surf. Sci. **401**, 199 (1998).

[13] J. P. Aimé, R. Boisgard, L. Nony, and G. Couturier, Phys. Rev. Lett. **82**, 3388 (1998).

[14] T. Albrecht, P. Grütter, D. Horne, and D. Rugar, J. Appl. Phys. **69**, 668 (1991).

[15] B. Gotsmann, D. Krüger, and H. Fuchs, Europhys. Lett. **39**, 153 (1997); *ibid.* **41**, 581 (1998).

[16] B. Gotsmann, B. Ancykowski, C. Seidel, and H. Fuchs, Appl. Surf. Sci. **140**, 314 (1999).

[17] B. Gotsmann, B. Ancykowski, C. Seidel, and H. Fuchs, Phys. Rev. B **60**, 11 051 (1999).

[18] see, e.g., Y. Martin, C. C. Williams, and H. K. Wichramasinghe, J. Appl. Phys. **61**, 4723 (1987); R. Erlandsson, G. M. McClelland, C. M. Mate, and S. Chiang, J. Vac. Sci. Technol. A **6**, 266 (1988); P. Grütter, H. J. Mamin, and D. Rugar, in *Scanning Tunneling Microscopy II*, edited by R. Wiesendanger and H.-H. Güntherodt (Springer, New York, 1992), pp. 151–207.

[19] H. Ueyama, Y. Sugawara, and S. Morita, Appl. Phys. A: Mater. Sci. Process. **A66**, S295 (1998).

[20] A. I. Livshits, A. L. Shluger, and A. Rohl, Appl. Surf. Sci. **140**, 327 (1999).

[21] F.-J. Giessibl, Phys. Rev. B **56**, 16 010 (1997).

[22] U. Dürig, Appl. Phys. Lett. **75**, 433 (1999).

[23] R. Peréz, I. Stich, M. C. Payne, and K. Terakura, Phys. Rev. B **58**, 10 835 (1998).

[24] M. Gauthier and M. Tsukada, Phys. Rev. B **60**, 11 716 (1999).

[25] U. Dürig, New J. Phys. **2**, 5.1 (2000).